Neuroscience 154 (2008) 10–21

THE DIMENSIONS AND STRUCTURAL ATTACHMENTS OF TIP LINKS IN MAMMALIAN COCHLEAR HAIR CELLS AND THE EFFECTS OF EXPOSURE TO DIFFERENT LEVELS OF EXTRACELLULAR CALCIUM

D. N. FURNESS,[a]* Y. KATORI,[b] B. NIRMAL KUMAR[c] AND C. M. HACKNEY[d]

[a]*Institute of Science and Technology in Medicine, School of Life Sciences, Keele University, Keele, Staffordshire, ST5 5BG, UK*

[b]*Department of Otolaryngology, Tohoku University School of Medicine, Sendai, 980-77, Japan*

[c]*Department of Otolaryngology, Head and Neck Surgery, Wrightington, Wigan and Leigh Hospital Trust, Royal Albert Edward Infirmary, Wigan Lane, Wigan, Lancashire WN1 2NN, UK*

[d]*Department of Physiology, Development and Neuroscience, University of Cambridge, Downing Street, Cambridge, CB2 3EG, UK*

Abstract—The tip links between stereocilia of acousticolateral hair cells have been suggested to contain cadherin 23 (CDH23) comprising an upper branched portion that is bound to a lower portion composed of protocadherin 15 (PCDH15). The molecular conformation of CDH23, its binding to PCDH15, the tip links, and mechanoelectrical transduction have all been shown previously to be sensitive to exposure to low levels of calcium. The aim of this study was to compare the characteristics of tip links in guinea-pig cochlear hair cells with reported features of the CDH23–PCDH15 complex. Tip links were examined using field emission scanning electron microscopy and transmission electron microscopy in conventional preparations and after treatment with the detergent Triton-X-100 or varying calcium concentrations in the extracellular solution. The results showed that tip links have a twisted double-stranded appearance with a branched upper region. They survived demembranation of the stereocilia by detergent suggesting that they have transmembrane domains at both ends. Their lengths, when fixed in the presence of 2 mM extracellular calcium, were ~150 nm. With prior exposure to 1 mM calcium their lengths were ~164 nm. The lengths in 50 μM calcium are similar (~185 nm) to those reported for CDH23–PCDH15 complexes in 100 μM calcium (~180 nm). Exposure to 1 μM calcium caused loss of tip links and an increased distance between the residual attachment sites. The data indicate that extracellular calcium concentration affects tip-link length. One model compatible with the recently proposed tip-link structure is that the CDH23 double strand undergoes calcium-dependent unfolding, changing the length of the links. The bundle may also tilt in the direction of the tallest row of stereocilia as the tip link lengthens and then is lost. Overall, our data are consistent with a tip link composed of complexes of CDH23 and PCDH15 but do not rule out other possibilities.

*Corresponding author. Tel: +44-1782-583496; fax: +44-1782-583496.
E-mail address: coa14@keele.ac.uk (D. N. Furness).

Abbreviations: CB, sodium cacodylate buffer containing 2 mM $CaCl_2$ at pH 7.4; CDH23, cadherin-23; FESEM, field emission scanning electron microscopy; MET, mechanotransduction; OTOTO, osmium-thiocarbohydrazide; PB, phosphate buffer; PBS, phosphate-buffered saline; PCDH15, protocadherin-15; TEM, transmission electron microscopy.

Key words: hearing, cochlea, stereocilia, mechanotransduction, adaptation, cadherin.

Vertebrate acousticolateral hair cells are mechanosensory cells with an apical bundle of stereocilia that increase in height stepwise across the bundle. They respond to sound-induced vibrations of the bundle; deflection toward the tallest stereociliary row causes an increase in the open probability of cationic mechanotransduction (MET) channels resulting in current flow and depolarization while deflection in the opposite direction decreases the open probability causing hyperpolarization (Corey and Hudspeth, 1979, 1983).

In mature hair cells, stereocilia are tethered to each other by extracellular row-to-row and side-to-side lateral links between their shafts (Bagger-Sjöbäck and Wersäll, 1973; Flock et al., 1977; Furness and Hackney, 1985; Neugebauer, 1986; Neugebauer and Thurm, 1987), by shorter tip connectors (Neugebauer and Thurm, 1987; Goodyear and Richardson, 1992) in a contact region with the adjacent stereocilium (Hackney et al., 1992; Hackney and Furness, 1995a), and by a distinct branched tip link that runs between the tip of each shorter stereocilium and the side of the next tallest stereocilium (Pickles et al., 1984; Furness and Hackney, 1985; Hackney and Furness, 1995a; Kachar et al., 2000). Electron-dense plaques occur at the upper and lower attachment sites of the tip link (Furness and Hackney, 1985).

The tip link has been suggested to represent a gating spring that operates the MET channels (Pickles et al., 1984) which may be located at one (Ricci et al., 1998) or both (Denk et al., 1995) ends of the link; tension in the tip link may increase for excitatory deflections but decrease for inhibitory directions thus modulating current flow through the MET channels. The MET currents also show calcium sensitive rapid adaptation on a sub-millisecond time scale and slower adaptation over tens of milliseconds (Ricci and Fettiplace 1997; Ricci et al., 1998). While fast adaptation may be intrinsic to the channel, the upper dense plaque appears to be enriched in myosin 1c (Garcia et al., 1998; Steyger et al., 1998) which could cause the plaque to move along the actin core and adjust the tension in the tip link to produce the slower component of adaptation (Hudspeth and Gillespie, 1994).

Investigation of the calcium sensitivity of transduction has shown that exposure of hair cells to low extracellular calcium levels simultaneously causes loss of MET and adaptation (Crawford et al., 1989), loss of the tip links and

0306-4522/08$32.00+0.00
doi:10.1016/j.neuroscience.2008.02.010

tilting of the bundle in the positive direction (Assad et al., 1991). Exposure of hair cells to calcium levels found in endolymph (approx. 50 μM) results in more channels being open at rest than exposure to the higher calcium concentrations of perilymph (Crawford et al., 1989) suggesting an increase in the open probability of the channels perhaps due to increased tension on the gating springs. The latter may thus give rise to changes in the appearance or dimensions of the tip link.

Structurally the tip link has the appearance of a braided inelastic macromolecule (Kachar et al., 2000) and appears to contain cadherin-23 (CDH23; Siemens et al., 2004) and protocadherin-15 (PCDH15; Ahmed et al., 2006), the former in the upper portion and the latter in the lower portion (Kazmierczak et al., 2007). Purified CDH23 also shows branching consistent with the morphology of the tip link, and it unfolds in the absence of calcium; it interacts with PCDH15 maximally at 0.1 mM calcium to form ~180 nm long heteromeric filamentous complexes (Kazmierczak et al., 2007).

In this study, structural features of the tip links, their attachment sites and their calcium sensitivity have been investigated further in the guinea-pig cochlea to evaluate their similarity to cadherins. Cadherins are typically composed of an ectodomain of a variable number of cadherin repeats, a transmembrane domain linking via a cytoplasmic domain often to the underlying cytoskeleton (Patel et al., 2003). Thus a cadherin-containing tip link might be expected to be firmly attached to the actin core of the stereocilium. The anchoring of the tip links to the cytoskeleton has therefore been explored using field emission scanning electron microscopy (FESEM) and transmission electron microscopy (TEM) of detergent-extracted samples where soluble components of the membrane are removed. The dimensions of tip links have been measured in a range of conventionally prepared specimens, and also some turtle material, to determine their similarity to CDH23-PCDH15 complexes. Finally, the structure and dimensions of tip links have also been assessed after exposure to different calcium concentrations to evaluate similarities to changes that might occur in a CDH23-PCDH15 complex.

EXPERIMENTAL PROCEDURES

Animals

Pigmented guinea pigs, weighing 400 g–850 g of both sexes (age range 6 weeks to 1 year), with normal Preyer reflexes, were used in this study (see below for numbers in each category). Previously resin-embedded basilar papillae from turtles of approximately 10 cm carapace length (n=2) were also used. All animals were killed with an overdose of pentobarbitone (200 mg/kg, i.p.) and decapitated, their temporal bones removed and the otic capsule opened to expose the cochleae for detergent treatment and fixation. A variety of different fixation solutions was used for both FESEM and TEM to obtain different kinds of structural information. Unless otherwise stated, in guinea-pig fixative solutions were gently perfused through the cochlear turns from a pipette via small holes made in the round window and apex. In turtles, the basilar papilla was pinned out in a dish and immersed in fixative. Fixation was carried out at room temperature. All experiments were conducted according to Keele University ethical guidelines and the UK Animals (Scientific Procedures) Act of 1986. The minimum number of animals was used to ensure appropriate statistical analysis would be performed and all possible steps were taken to minimize suffering.

Preparation of non-detergent treated samples for FESEM

For FESEM, guinea-pig cochleae (n=2) were fixed with 2.5% glutaraldehyde in 0.1 M sodium cacodylate buffer containing 2 mM $CaCl_2$ at pH 7.4 (CB) for 2 h. They were then processed using the osmium-thiohydrocarbozide (OTOTO) impregnation technique (Heywood and Resnick, 1981; Furness and Hackney, 1986). Briefly, after washing in CB, cochleae were post-fixed with 1% osmium tetroxide in CB for 1 h, the bony shell removed and the spiral organ dissected into segments. The segments were immersed in saturated thiocarbohydrazide(aq) for 20 min, washed six times with distilled water, placed in 1% osmium tetroxide in CB for 1 h and washed six times as before. These steps were repeated twice to increase the electron conductivity of the specimens. Segments were then dehydrated in a graded series of ethanol solutions, critical point dried using liquid carbon dioxide as the transitional fluid, mounted on specimen stubs using silver electroconductive paint and viewed using a Hitachi S-4500 FESEM operated at 3–20 kV.

Preparation of non-detergent treated samples for TEM

Two initial fixatives were used for conventional TEM. Cochleae were either fixed with 2.5% glutaraldehyde in CB for 2 h (n=4) or with 2.5% glutaraldehyde in CB for 1 h followed by 1 h in the same fixative containing 1% tannic acid (n=2). After washing three times in CB, all cochleae were post-fixed with 1% osmium tetroxide in CB for 1 h, washed and dissected into segments which were dehydrated in a graded series of ethanols and embedded in Spurr (Agar Scientific, Stansted, UK) or Durcupan resin (Fluka Chemie, Buchs, Switzerland). Ultrathin sections (approx. 70–100 nm) were cut on a Reichert Ultracut E microtome, stained with ethanolic uranyl acetate and lead citrate, and examined in JEOL IOOCX or JEOL1230 TEMs operated at 100 kV. Photographic images were acquired on Ilford EM film or digital images were acquired using a MegaView III digital camera using analySIS® software.

Detergent treatments

Triton-X-100 (Sigma-Aldrich Chemical Co, St. Louis, MO, USA) was used to extract lipid components and detergent soluble proteins from the stereociliary membrane to reveal cytoskeletal attachments and enhance features of the linkage attachment site. Three combinations of detergent treatment and initial fixation were used and the most useful repeated as necessary (see Table 1 for numbers of experiments and conditions):

Prefixation detergent treatment. Cochleae were dissected in 0.15 M phosphate-buffered saline (PBS, pH 7.4) to allow exposure to detergent prior to fixation. The bony shell, spiral ligament,

Table 1. Summary of the different detergent treatments and number of experiments used in this study

%Triton-X-100	0.01	0.05	0.25	0.4	1	1.25	2.5	Total
Before fixation	1	1	3		1			6
During fixation	1	1	1	1	4	1	7	16
After fixation							4	4

Values are the number of experiments in each condition.

and stria vascularis of each turn were quickly removed and the exposed spiral organs were incubated in Triton-X-100 in PBS for 10 min followed by washing in PBS;

Simultaneous fixation and detergent treatment. Cochleae were fixed with 4% paraformaldehyde in 0.1 M sodium phosphate buffer (PB, pH 7.4) containing Triton-X-100 for 2 h and washed with PBS.

Post-fixation detergent treatment. Cochleae were fixed by perfusion with 4% paraformaldehyde in 0.1 M PB (pH 7.4) for 2 h, washed with PBS, immersed in Triton-X-100 in PBS for 30 min and then washed in PBS.

After each of these treatments, further fixation with 2.5% glutaraldehyde in CB took place and samples were then processed as described above either using the OTOTO method followed by dehydration and critical point drying for FESEM or post-fixation in 1% OsO_4 in CB, dehydration and embedding in Spurr resin for TEM.

Measurement of tip-link dimensions

Tip-link lengths after conventional fixation for TEM were obtained from two different sources: (i) our archive of electron micrographs where various different preparations, magnifications and cochlear locations have been used, and (ii) a more standardized set from outer hair cells in a mid-apical cochlear location, fixed with 2.5% glutaraldehyde in CB for 1 h followed by 1 h in the same fixative containing 1% tannic acid, and post-fixed in 1% osmium tetroxide, dehydrated and embedded in Spurr resin. The full length of a tip link is only visible in TEM in radial sections but, the branching is usually obscure; thus the lengths are measured from the tip of the short stereocilium to the midpoint of the upper dense plaque. This may not represent the length of the tip link directly but is a close approximation.

Exposure of hair cells to different calcium conditions

To examine the effects of changing calcium concentration on the structure of tip links, 12 cochleae from 12 guinea pigs were obtained as before. Only one cochlea was used from each to minimize postmortem pathological changes caused by delayed exposure. The other cochlea was fixed for conventional electron microscopy. Each experimental cochlea was placed in Hanks' buffered salt solution (HBSS), chilled to reduce changes in ionic distribution that may occur *in vitro*, opened, and the central modiolus broken across at its base. The spiral was dissected out and incubated for 20 min in one of three different artificial perilymph solutions:

(i) 1 mM Ca^{2+} composed of (in mM) NaCl (142), KCl (4), $MgCl_2$ (1.5) and $CaCl_2$ (1)
(ii) 50 μM Ca^{2+} composed of NaCl (136), KCl (4) and $CaCl_2$ (0.05)
(iii) 1 μM Ca^{2+} composed of NaCl (142), KCl (4), $CaCl_2$ (2.5) and Na-HEDTA (5)

In addition, each solution contained 5 mM Na-Hepes and 4 mM glucose. The calcium concentrations were checked with a calcium electrode (thanks to assistance from Professor Andrew Crawford, Department of Physiology, Development and Neuroscience, University of Cambridge).

Cochleae were then fixed by direct immersion in 2.5% glutaraldehyde in CB for 2 h and prepared either for FESEM (n=1 for each condition to evaluate tip link survival) or TEM (n=3 from each condition to analyze the structure and dimensions of tip links) as described above.

For FESEM, 10 hair bundles were selected for each condition from approximately equivalent locations on the cochlear spiral using low magnification so that hair-bundle choice was not biased by tip-link presence or absence. The magnification was then increased to ×40,000 and an image acquired of each bundle for counting tip links.

For TEM, ultrathin sections were acquired from mid-apical locations in each of the three samples for each condition and stained as before. Images were recorded on Ilford EM film at ×14,000 of pairs of stereocilia of the tallest and next tallest row from outer hair cells in row 1 only (to maximize uniformity). For inclusion for measurement, each stereociliary pair had to be full length (as indicated by the presence of electron dense caps at the tips and ankles at the base) and to contain identifiable tip-link attachment sites. For the 1 mM and 50 μM calcium condition, measurements were only taken if a clear tip link was identifiable. For the 1 μM condition, tip links were largely absent and so that criterion could not be met. However, bundles where stereocilia were obviously bent or damaged were not selected for measurement.

Micrographs were also taken of the tip-link region at a magnification of ×72,000. The lengths of the stereocilia (Lt and Ls) and the proportional distance of the upper dense attachment site from the tip of the stereocilium in which it was located (p) were measured in the lower power micrographs; the dimensions of the right-angled triangle made by the tip link's lower and upper attachment points, the tip of the shorter stereocilium and the side of the tall stereocilium were determined from the higher power pictures (n=20 in each sample). Measurements were made directly from the negatives using a graduated eyepiece. The microscope magnification was calibrated periodically to check for consistency using a cross-grating grid with 2160 lines/mm.

Statistical analysis of the data were performed either using Microsoft Excel (parametric tests only) or manually (non-parametric tests).

RESULTS

Morphology of the extracellular cross links

Tip links were found connecting the tips of the majority of shorter stereocilia with the sides of adjacent taller stereocilia in many well-preserved hair bundles in OTOTO preparations following conventional glutaraldehyde fixation (Fig. 1A). They typically had a Y-shaped morphology, with a single strand emanating from the tip of the short stereocilium branching into two strands attaching to the taller stereocilium.

The morphology of the tip links after fixation with formaldehyde followed by OTOTO was then investigated as the effects of Triton-X-100 were subsequently determined in formaldehyde fixed samples where proteins are less well preserved. The stereocilia after formaldehyde fixation had rougher surfaces but tip links were similar in morphology to those observed after glutaraldehyde fixation (Fig. 1B).

At higher magnifications, more details of the tip link could be seen. Those which were forked consisted of a single strand forming the lower portion branching into two, one half to two thirds (approximately) of the distance toward the upper attachment (Fig. 1C). In FESEM, each of the two branches was often similar in width to the lower single filament. In some cases, tip links had a twisted double-stranded appearance (Fig. 1D). Sometimes tip links were less obviously branched appearing as a relatively featureless single strand but widening at the upper end suggesting shortened branches (Fig. 1E).

Lateral links were also visible between stereocilia, most obviously in outer hair cells where they form bands

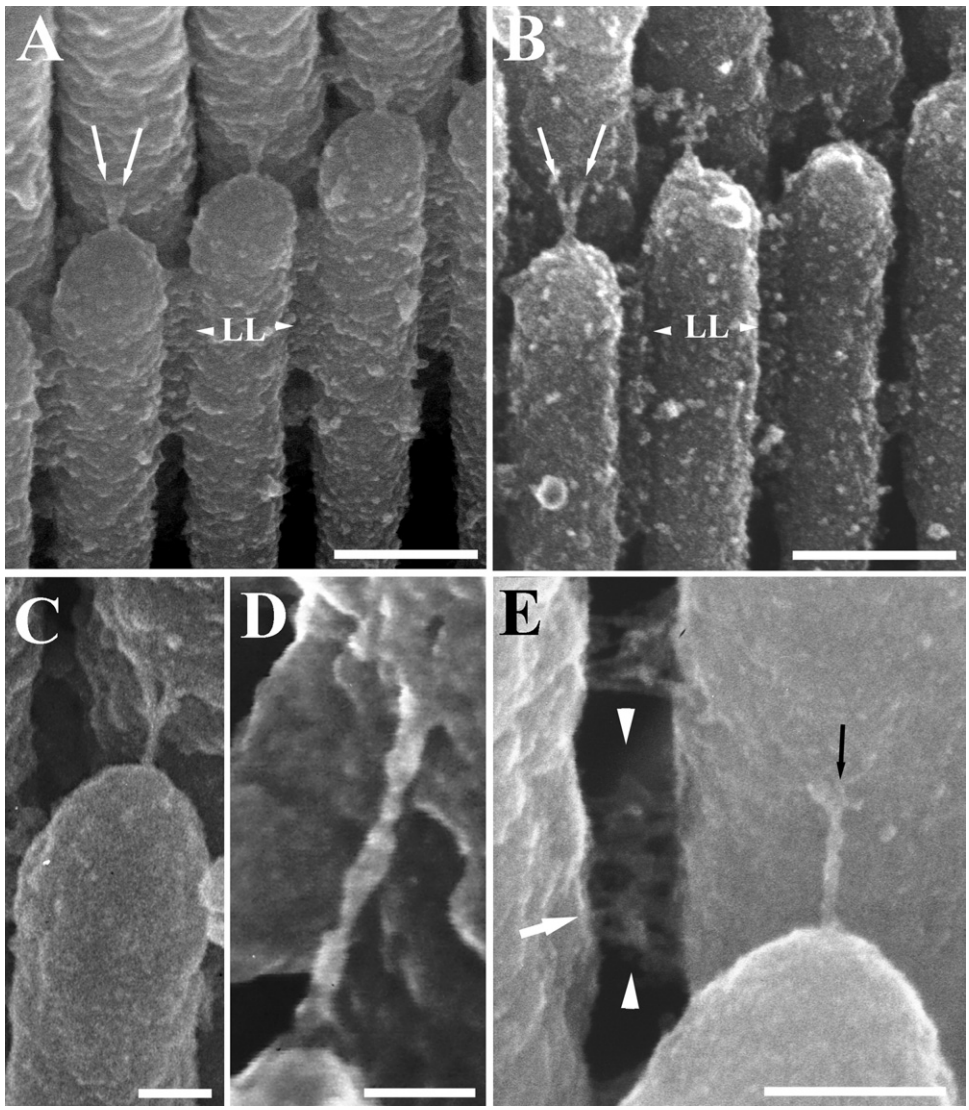

Fig. 1. (A) Field emission scanning electron micrograph showing the stereocilia and extracellular cross-links after glutaraldehyde fixation and preparation by the OTOTO method. The stereociliary membranes are intact and show a degree of surface roughness. Tip links are visible at the tips of most of the shorter stereocilia and are typically branched (arrows), as shown at a higher magnification in (C). Lateral links (LL) also connect the adjacent stereocilia. (B) Tip-link morphology after fixation with formaldehyde. The links are similar to those seen after glutaraldehyde fixation but the membrane appears rougher (arrows show branches, LL indicate lateral links). (C) Detail of a tip link showing two branches. (D) Example of a tip link showing the twisted double strand conformation. (E) Example of a tip link where it widens at its upper end but does not clearly show branching (black arrow). Details of the lateral links are also visible, with strands (e.g. white arrow) emanating from each adjacent stereocilium and joining in the middle where globular material is present (between arrowheads). Scale bars=250 nm (A, B); 50 nm (C, D); 100 nm (E).

best seen along the shortest row of stereocilia. However, they were also present between the stereocilia of other rows. Mild detergent treatment after formaldehyde fixation sometimes enhanced these links so that the fine strands emanating from the membrane could be seen to join larger globular material near the middle of each band (Fig. 1E).

Effects of detergent extraction

The effects of treatment with Triton-X-100 depended upon the strength of the detergent solution and the point at which exposure to it occurred. Exposure to 0.25% detergent prior to fixation resulted in removal of much of the stereociliary membrane but left the actin core with a coating of filamentous and globular material. The membrane tended to be preserved well only in the ankle regions of the stereocilia. Occasionally, the parallel actin filaments could be seen but more often, as shown in Fig. 2A, they were obscured by overlying material. Similar results were obtained with exposure to higher levels of Triton-X-100 (1.25%) during fixation but with less disorder of the stereocilia (Fig. 2B). Treatment with 2.5% Triton-X-100 after fixation resulted in stereocilia which were well ordered and coated with many globular patches (Fig. 2C).

Both tip links and lateral links were still present to varying extents after all the different detergent treatments. Observations using FESEM showed that treatment with

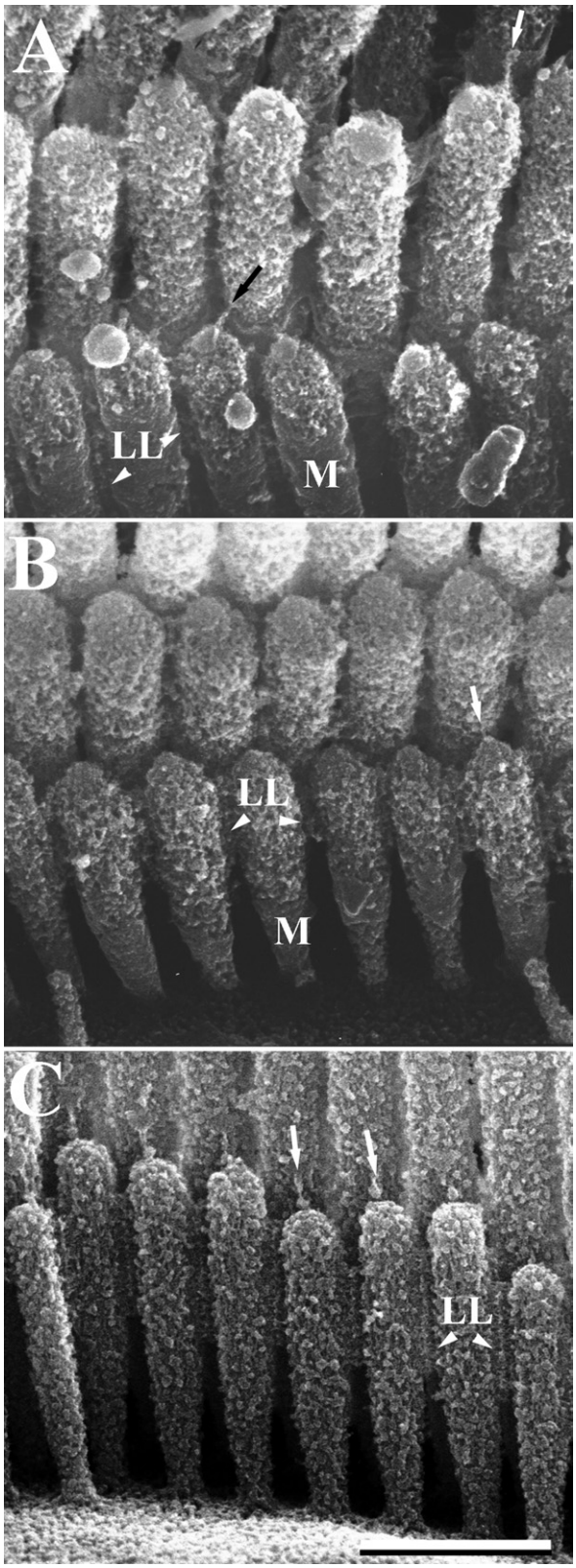

Fig. 2. Effects of various different Triton-X-100 treatments on stereociliary appearance. (A) Treatment with 0.25% Triton-X-100 prior to fixation substantially removes the membranes, leaving some residual membrane around the lower shaft (M). Lateral links (LL) and tip links (arrows) are still present in places. (B) Treatment with 1.25% Triton-X-100 during fixation has similar effects as 0.25% prior to fixation (labels as in A). (C) Treatment with 2.5% Triton-X-100 after fixation appears to remove more of the membrane but preserves more links. Arrows show tip links, some of which have globular material near their lower end; LL indicates lateral links. Scale bar=600 nm.

0.25% Triton-X-100 before fixation left several surviving tip links on a bundle (Figs. 2A, 3A, B). Treatment with higher concentrations prior to fixation caused more damage and preservation of the links was not apparent. Treatment with weak Triton-X-100 solution (0.01%) during fixation (Fig. 3C) left many more tip links visible compared with any treatment prior to fixation and the branched region could be clearly seen. The effect of stronger detergent treatment during fixation was an increasingly greater apparent removal of the stereociliary membrane as detergent strength increased, leaving the tip link and its upper attachment site visible as a plaque on the lateral wall of the stereocilium especially after the highest concentrations used (Fig. 3D). The tip link often was attached to a globular structure at the lower end after 2.5% Triton-X-100 treatment following fixation (Fig. 3E).

Observations using TEM were focused on the most effective Triton-X-100 treatment (2.5% during fixation). When compared with preparations made without using detergent (Fig. 4A, C), this treatment resulted in significant loss of membrane as judged by the absence of clear bilayer structures (Fig. 4B, D) although amorphous material visible could have been remnants of the membrane that were resistant to detergent. The tip links (Fig. 4B) and lateral links (Fig. 4B, D) both survived detergent treatment and TEM embedding.

When compared with the structure of the tip link in conventional material (Fig. 5A) more details were visible after detergent treatment (Fig. 5B). The tip link had a filamentous appearance with branches visible as it approached both the upper and lower attachment sites. The attachment sites also retained their electron density (Fig. 5B). The branching filaments at either end appeared to connect directly with the dense plaques. This arrangement is only visible at the lower attachment site after demembranation has occurred. Some evidence of this branching may be represented by the strands emanating from the globular material at the lower end of the tip link visible with FESEM after detergent treatment (Fig. 3E).

Substructure of the dense attachment sites

The attachment sites at the upper and lower end of the tip link both contain electron dense material in conventional preparations for TEM. When enhanced by tannic acid, the plaques were more obvious, but showed less substructure. The upper plaque tended to coincide with an indentation of the membrane, and the tip link usually inserted into the lower half of this plaque. The lower plaque often had a very regular rectangular shape (Fig. 4A). Tannic acid also made the contact region denser and more obvious (Fig. 4A, inset).

The lower dense material seemed to consist of granular material in some sections, although little detail of its

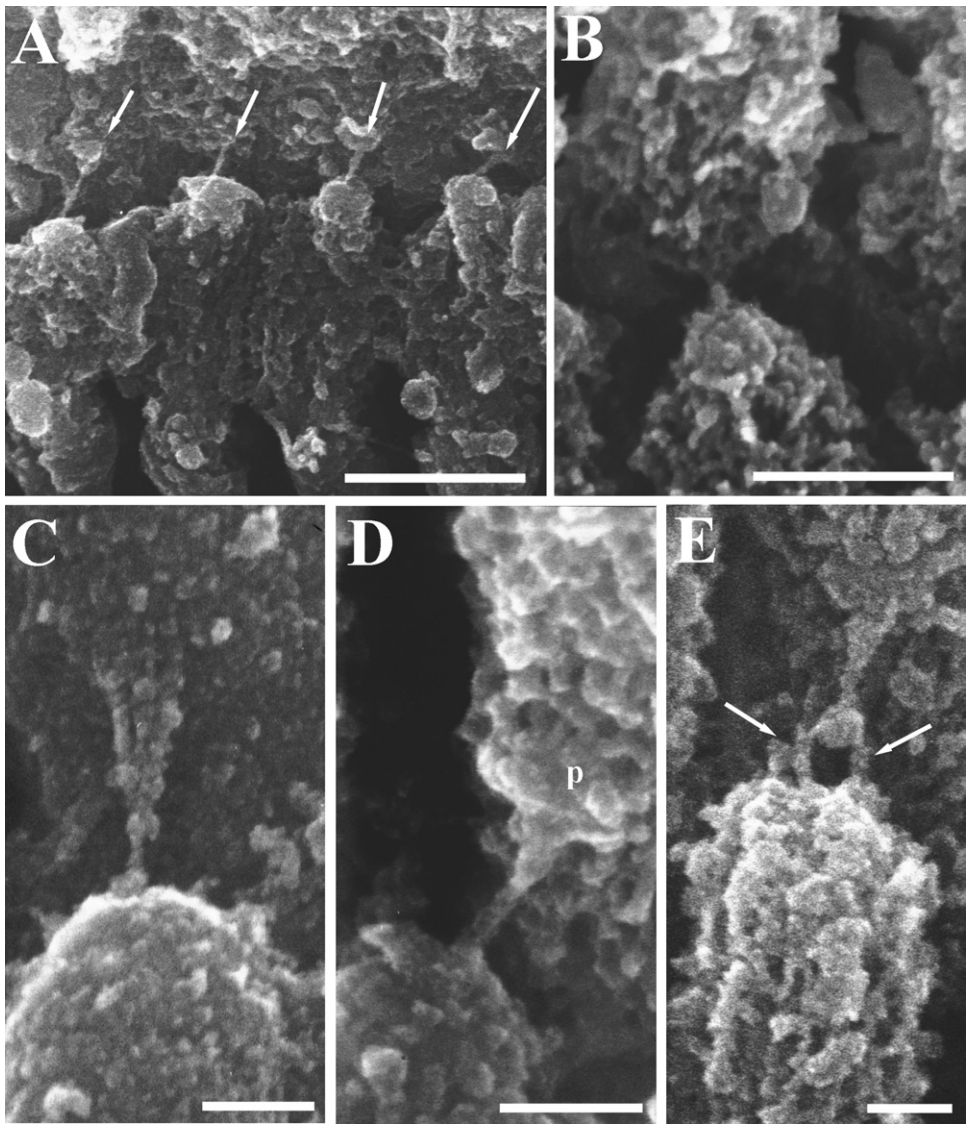

Fig. 3. Effects of various different Triton-X-100 treatments on tip link appearance. (A) After treatment with 0.25% Triton-X-100 prior to fixation the tip links (arrows) appear attached to the stereociliary core. Branching is not readily distinguished. Treatment with 1.25% (B), 2.5% (C) during or 2.5% Triton-X-100 (D) after fixation leaves tip links attached often with a plaque visible at the upper attachment site (P in D). In (C) there may be three strands above the branch point. (E) 2.5% Triton-X-100 after fixation produces tip links with globular material at the lower end from which strands connect to the tip of the shorter stereocilium (arrows). Scale bars=300 nm (A); 180 nm (B); 50 nm (C–E).

organization could be discerned. The upper dense material frequently showed evidence of a substructure composed of several globular or ring-like structures, best seen when tannic acid was not present. The number of these structures was variable. These were visible either as black or white annular or polygonal structures in conventionally prepared material (Fig. 5A) with overall diameters of about 10–15 nm and central cores approximately 5 nm in diameter.

To determine whether more details could be obtained from the electron micrographs of the dense plaque and ring-like substructures, images were digitized and enhanced using unsharp-mask filtering using Adobe Photoshop®. This enabled clearer visualization of the regular polygonal shape of one of these particles (Fig. 5 inset) and enhanced other particles in the plaque.

Tip-link length

Tip-link lengths were measured from our archive of micrographs from four different guinea-pig samples and two turtles as summarized in Table 2 and Fig. 6. The mean ±S.D. of guinea-pig tip link lengths was 142±26 nm (n=20). The maximum length measured was 190 nm (2 tip links) and the minimum 90 nm (1 tip link), both measurements having been obtained from the same sample (Table 2). For comparison, tip links in turtle samples were 143±24 nm (n=6).

To obtain lengths more systematically, a set of micrographs taken at ×48,000 or ×58,000 only of guinea-pig outer hair cells in one cochlear location was analyzed (Fig. 6). These gave a mean of 155.7±13 nm (n=26) and range

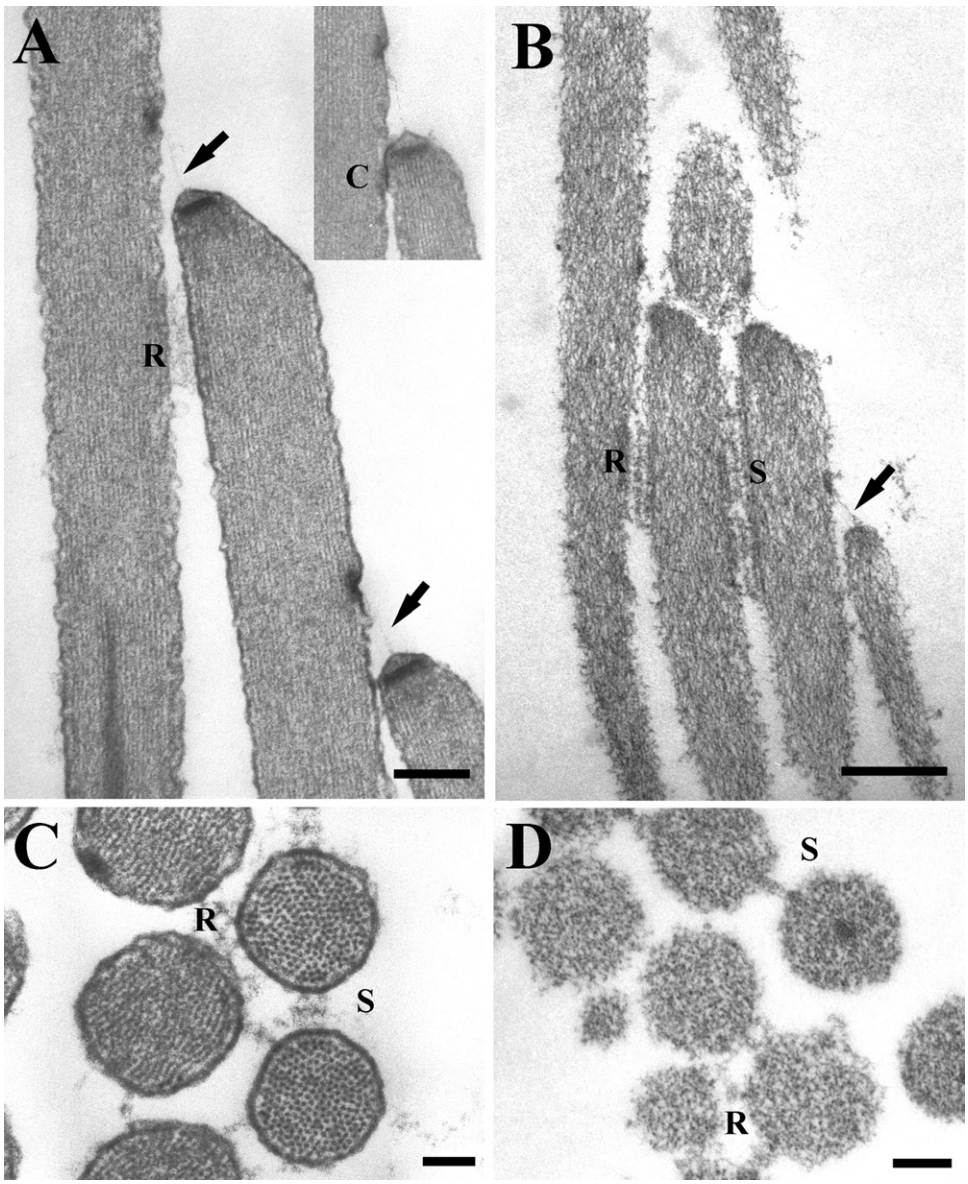

Fig. 4. TEM of stereocilia in conventionally prepared material (A, C) and after 2.5% Triton-X-100 treatment following fixation (B, D). Tannic acid was also included in the fixatives. (A) An example of two tip links in the same radial section between stereocilia of the tallest and intermediate rows, and intermediate and shortest rows. The tip links (arrows) and their associated upper and lower dense plaques appear similar and are of similar length in the two pairs. Note also the row-to-row lateral links (R). The inset shows the contact region (C) in a similar section. (B) After Triton-X-100 row-to-row (R) and side-to-side (S) lateral links, tip links (arrow) and their attachment sites are all clearly visible even though most of the membrane has been removed. (C). Horizontal section showing the conventional appearance of row-to-row (R) and side-to-side (S) lateral links. (D) Horizontal section showing both orientations of lateral link are present after detergent treatment (labels as in C). Scale bars=200 nm (A, B); 100 nm (C, D).

of minimum to maximum of 127.5–187.5 nm. The data were further subdivided into links between tall and intermediate stereocilia (156.3±15 nm, $n=15$) and links between intermediate and short stereocilia (154.9±11 nm, $n=11$). No significant difference was detected between the two categories of tip link ($P=0.79$, two-tailed Student's *t*-test).

Effects of exposure to different calcium concentrations

The number of tip links surviving after treatment with different calcium concentrations was determined from specimens prepared for FESEM. Only one sample was prepared for each condition as the primary purpose was to confirm that the 1 μM calcium solution eliminated the tip links. In 10 hair bundles from each sample, visibly intact tip links were common in the AP condition (percentage of possible locations containing a tip link=52%), fewer in 50 μM calcium (41%) and least common in the 1 μM calcium (5%), confirming that tip links are largely destroyed in the lowest calcium condition. Broken tip links and stumps of tip links were also observed, to a greater extent in 50 μM calcium (30%) compared with AP (15%) and 1 μM calcium (9%).

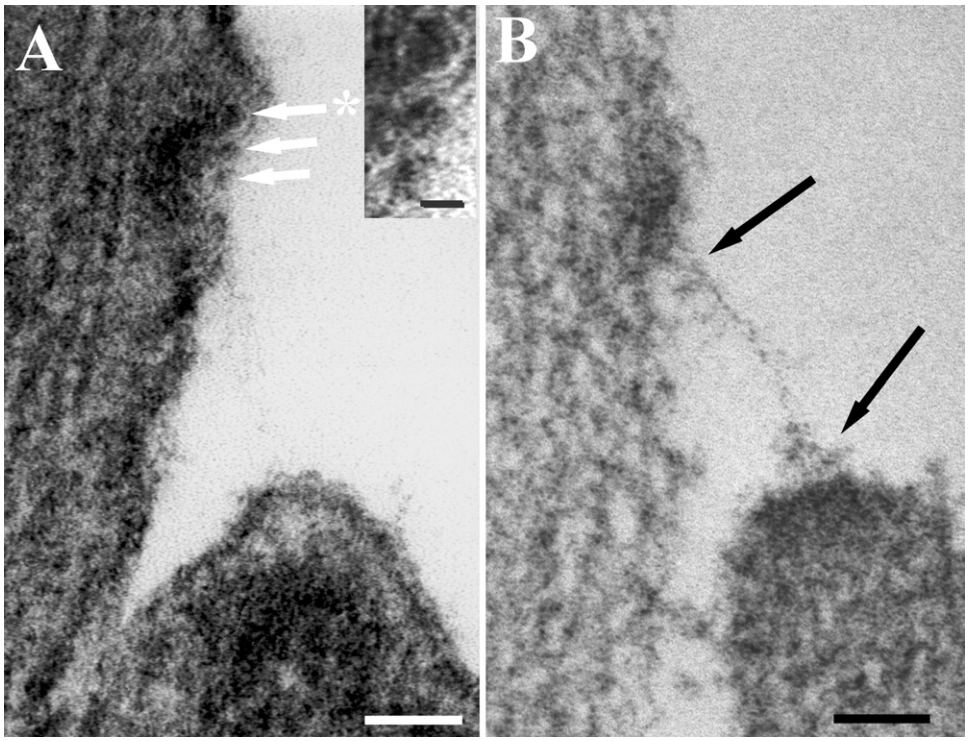

Fig. 5. Details of tip-link structure in TEM. (A) The upper dense plaque appears to contain a number of dense subunits. The arrows indicate three that are shown enlarged in the inset, which has been filtered using the unsharp mask function in Adobe Photoshop® in order to make the individual particles clearer. (B) After detergent treatment (2.5% Triton-X-100 post-fixation), membranes have been removed and the tip link shows branches at either end where it approaches the electron dense plaques (arrows). The dense plaques are relatively unaffected by the detergent treatment. Scale bars=50 nm (A, B) 10 nm (inset).

The structural and geometrical changes that occurred in different calcium conditions were determined by TEM. In the two higher calcium conditions, tip links were frequently visible, and the tips of the shorter stereocilia appeared tented with a distinct gap between the membrane and the dense cap over the actin core. In 1 μM calcium, the tip links were absent and the gap between the dense material and the membrane at the tip of the shorter stereocilium was reduced, the tips themselves becoming more rounded. No alterations were noted in the substructure of the dense material of either attachment site, both of which were still retained when tip links were absent (Fig. 7).

Measurements of the proportional distance (p) of the upper attachment site from the tallest stereociliary tip were 0.334 ± 0.014 in AP, 0.359 in 50 μM calcium and 0.325 in 1 μM calcium. These values were not significantly different and showed no obvious trend. The distances between the upper and lower attachment points of the tip link were 164.4 ± 57.3 nm in AP, 185.8 ± 37.6 nm in 50 μM calcium and 209.7 ± 38.9 nm in 1 μM calcium (Fig. 6B). The first two measurements represent the lengths of the tip link in the two different conditions. A Kruskal-Wallis test showed that there were significant differences between the treatments ($P=0.0118$) while Dunn's multiple comparison post testing revealed that they reached significance ($P<0.05$) only between AP and 1 μM calcium condition. The difference between mean lengths of the tip link in AP and 50 μM calcium was approximately 13%.

DISCUSSION

The aim of this study was primarily to investigate attachments of the tip link, tip-link dimensions and sensitivity to calcium for comparison with recent reports on the properties of PCDH15 and CDH23, possible components of the tip link.

Attachment of the links to the cytoskeleton

The present results show that the tip links and their dense attachment material resist detergent extraction thereby suggesting a relatively firm attachment to the cytoskeletal cores of both stereocilia. This implies that there are transmembrane domains at the ends of the tip link or that the link binds strongly to transmembrane proteins attached to the cytoskeleton, perhaps represented by the submembrane strands emanating from its lower end (Osborne et al., 1988; Kachar et al., 2000). These observations are consistent with the tip link being composed of cadherins but with the caveat that other molecules may also fulfill these conditions.

As reported by Flock et al. (1977), the lateral links also remain attached after detergent treatment. Together with the tip-link data, this implies that intracellular processes could alter the interaction of extracellular links with the

Table 2. Dimensions of tip links in various samples and preparation conditions

HC type	Type	Length, nm	Sample identity and, if known, cochlear location	Resin
OHC	SI	136.36	DZ1	Durcupan
OHC	TI	142.42	DZ1	Durcupan
OHC	SI	121.21	DZ1	Durcupan
OHC	TI	136.36	DZ1	Durcupan
OHC	TI	128.79	DZ1	Durcupan
IHC	SI	128.79	DZ1	Durcupan
IHC	TI	128.79	DZ1	Durcupan
IHC	SI	128.79	1043, Mid region	Spurr
IHC	SI	163.64	1043, Mid region	Spurr
IHC	SI	130.00	1043, Mid region	Spurr
IHC	SI	130.00	1043, Mid region	Spurr
IHC	SI	180.00	1043, Mid region	Spurr
IHC	SI	127.27	1043, Mid region	Spurr
OHC	TI	160.00	1151c, Mid region	Spurr
OHC	SI	170.00	1151c, Mid region	Spurr
OHC	TI	121.21	1153c, Basal region	Spurr
OHC	TI	190.00	1153c, Basal region	Spurr
OHC	TI	190.00	1153c, Basal region	Spurr
OHC	SI	90.00	1153c, Basal region	Spurr
OHC	TI	151.52	1153c, Basal region	Spurr
		150.00	Turtle 4R	Spurr
		175.76	Turtle 4R	Spurr
		163.64	Turtle 4R	Spurr
		136.84	Turtle 3L	Spurr
		113.64	Turtle 3L	Spurr
		121.21	Turtle 3L	Spurr

The hair cell type (OHC=outer hair cell, IHC=inner hair cell), the rows which are connected (TI=tall to intermediate, SI=short to intermediate), the length in nm, the sample identity in our database and location along the cochlea (if known) and the resin used to embed the sample are given.

cytoskeleton to modify bundle properties. Calmodulin is enriched in both the upper and lower attachment site of the tip links and where lateral links attach (Furness et al., 2002) making these potential sites for modulation of the attachment by calcium.

Myosin 1c in the upper attachment plaque of the tip link (Steyger et al., 1998) has been proposed to form the slow adaptation motor. One question, therefore, is whether the structure of the attachment sites is consistent with them containing myosin. While the lower attachment site was homogenous, 10–15 nm diameter substructures were visible in the upper dense plaque. These may be larger than expected for myosin 1c; the similar myosin 1b has a head domain with a radius of about 8 nm (Stafford et al., 2005) and their sometimes polygonal shape is reminiscent of a channel. However, while TEM can be used to visualize some channel structure (Unwin, 2003), the present images are too ambiguous to interpret these structures as channels or as myosin molecules.

If the upper plaque contains the adaptation motor, it has been predicted to slip down when the tip link is under tension and climb to restore tension after deflection of the stereocilia (Assad and Corey, 1992). We looked for relative movement of the plaque in the presence and absence of tip links where tension would be relieved but could detect no significant change in its proportional distance from the tip of the stereocilium in which it was located.

Dimensions of tip links

The length of the tip links measured in our conventional samples was ~150 nm, ranging from 90 nm (one tip link) to 190 nm (two tip links). This range is considerable, and the mean is shorter than the predicted length for CDH23 and PCDH15 associations of ~180 nm (Kazmierczak et al., 2007). The variability may arise from a number of sources.

Measurement error. First, it is difficult to determine the precise ending of the tip link in TEM. To reduce this error, the mid-point of the upper dense plaque and the tip of the shorter stereocilium were consistently used. However, if the link attaches either to the top or bottom of the dense plaque, the error would be (at most) 25 nm or half the width of the plaque. Frequently, the link attached to the lower half of the plaque making the lengths we have measured overestimates rather than underestimates.

Second, the link could lie obliquely in section generating a parallax error. In ~100 nm thick sections, a 180 nm obliquely oriented tip link viewed laterally would appear to be 160 nm long, closer to our mean values. However, since measurements were made on sections containing significant portions of the full length of the stereocilia, the long axes of the tip link would normally be parallel to the section face. Thus few tip links would be oblique and the contribution of parallax error to mean tip-link length small. Moreover, the minimum length (90 nm), when corrected for maximum parallax error, would represent a 135 nm long tip link which is still too short by 25%; while this may have been anomalous, the next highest value was ~120 nm which

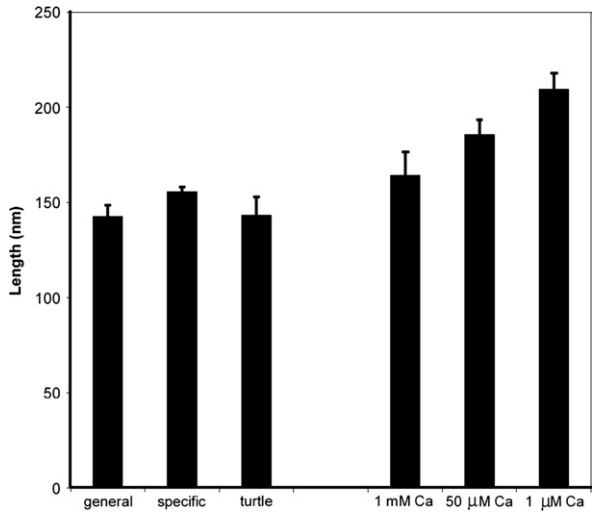

Fig. 6. Histogram showing the distance between the tip-link attachment sites in various samples: on the left half of the histogram, 'general' refers to our archive of micrographs; 'specific' refers to one sample of mid-apical outer hair cells and 'turtle' refers to micrographs from turtle samples. On the right-hand side, the distance in different calcium concentrations is shown. Note that as calcium concentration decreases, the distance increases. Values represent the mean and standard error.

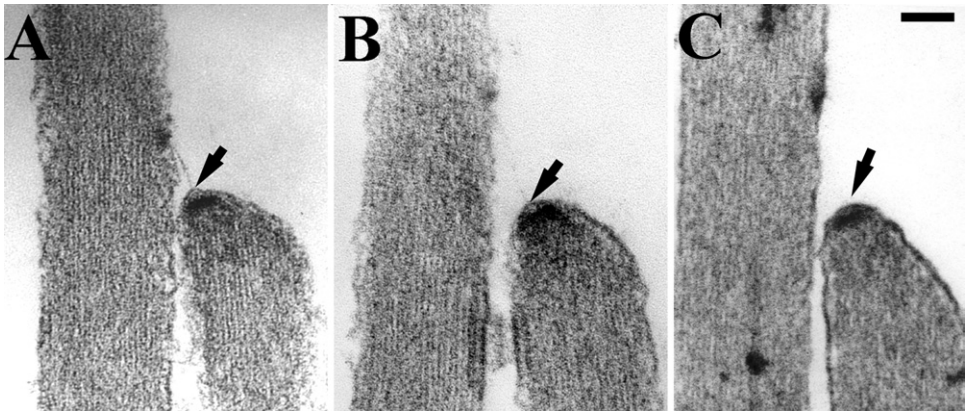

Fig. 7. The ultrastructure of the tip-link region after exposure to different calcium concentrations. After incubation in artificial perilymph containing 1 mM calcium (A) or 50 μM calcium (B), the tip link has a normal morphology. The tips of the short stereocilia are slightly tented (arrows) and there is a gap between the dense material and the membrane. After 1 μM calcium (C) the tip link is absent and the short stereocilium tip is rounded with a less obvious gap between the membrane and the dense cap. Scale bar=50 nm.

would represent a maximum of 156 nm, still 13% shorter than the 180 nm cadherin complex.

Third, there could be shrinkage of the tissue in preparation for TEM, causing the gaps between stereocilia to narrow, shortening the link. However, the fact that the lengths can vary by at least 30% (and possibly as much as 100%) in the same sample would probably rule out shrinkage as a major factor in the variability.

Thus overall, the measurement errors may account for some of the apparent variability of tip-link length, but much of it is also likely to be due to other factors.

Variation in tip-link composition. If it is made of a CDH23–PCDH15 complex, could differences in the number of residues or of molecules of each cadherin explain tip link length variations? CDH23 normally has 27 cadherin residues in the ectodomain (Sotomayor et al., 2005), while PCDH15 has 11 (Ahmed et al., 2006). The data presented here are not sufficiently high resolution to determine whether residue number varies, but it seems unlikely that variations in the number of molecules occur since the lengths were continuously variable rather than forming discrete groups as would be expected.

The identical morphology (Furness and Hackney, 2006) and similar mean lengths of turtle tip links suggest a highly conserved composition. Similarly, avian tip links are between 150–200 nm long (Tsuprun et al., 2004). Although the latter are longer overall than in our conventional material, the calcium concentration present in the preparation of the avian material was not specified by the above authors and this could affect the lengths obtained (see below).

Physiological variation in tip links. The best agreement between tip-link length and the length of the CDH23–PCDH15 complexes was that found after the 50 μM calcium exposure ($\sim$185 nm vs. 180 nm). Among our conditions, this was closest to the optimal 100 μM calcium needed for formation of the complex (Kazmierczak et al., 2007) suggesting physiological conditions affects the link dimensions. The tip-link length data presented here can be best reconciled with the data from CDH23–PCDH15 preparations if the molecular organization of the tip link is calcium-dependent.

The effects of calcium on tip-links and their length

Survival of tip links in different extracellular calcium concentrations. Observations using FESEM confirmed that tip links were largely absent after removal of calcium, and that in 50 μm calcium, more were broken than in 1 mM calcium. Even in the latter, only 50% of possible tip locations contained identifiable tip links. Variability in tip-link numbers in other preparations (Furness and Hackney, unpublished observations) suggests that it is rare that all tip links are preserved, so the 50% observed in 1 mM calcium reflects an element of survival of the preparation.

Dimensions of tip links in different extracellular calcium concentrations. Decreases in calcium concentration appeared to systematically increase tip-link length and separation of the attachment sites. One explanation of this observation is that the molecular conformation of the tip link is modified by the changes in calcium ion concentration. A mechanism for the length change may be the tip link unfolding at its branch point. This is possible because observations on tip-link structure suggest either a double (Kachar et al., 2000; Tsuprun et al., 2004) or triple (Tsuprun and Santi, 2000) helical structure that could unwind. Different degrees of unfolding may explain the variability of lengths obtained across all our samples and result in the ultimate loss of the link.

This view is consistent with the appearance of cadherin 23 in trans which has branches of variable length reminiscent of different degrees of unfolding (Kazmierczak et al., 2007). The absence of branching in some tip links supports the idea that the degree of unwinding is variable. Since cadherin 23 unfolds in the absence of calcium (Kazmierczak et al., 2007) this could also explain the increased length with decreased calcium if the unfolding is facilitated by partial removal of calcium ions.

Another explanation for the length change is that the stereocilia become displaced in an excitatory direction in

low extracellular calcium as has been observed in bullfrog (Assad et al., 1991) and turtle (Hackney and Furness, 1995b). If the displacement increases with decreasing calcium then elongation and eventual loss of the tip links would occur as the tension on the link increases until it breaks. This is also suggested by the rounding of the stereociliary tips after loss of the tip link indicating removal of tension (Hackney and Furness, 1995b; Rzadzinska et al., 2004), by the greater proportion of broken links in 50 μM calcium than in AP, and by the reduced gap between the membrane and dense material in the shorter stereocilium after 1 μM calcium treatment. Since there are observations which support both the unfolding and the displacement suggestions, it could also be that the two combine to generate the results observed here.

Is there an alternative mechanism to these two hypotheses? Molecular modeling studies by Sotomayor et al. (2005) suggest that cadherin would require a physiologically unlikely force to stretch the molecule by 10 nm. The apparent change in length found here of about 13% or 20 nm from a resting length of 165 nm, in conditions between 1 mM and 50 μM calcium where the transduction mechanism still functions, is thus less consistent with a simple physical stretching of the tip link assuming that it is composed of cadherin molecules.

CONCLUSIONS

The data presented here indicate that the tip links have trans-membrane domains consistent with a cadherin-based composition. Tip-link lengths can be reconciled with the size of CDH23–PCDH15 complexes in appropriate calcium conditions. The changes detected in different extracellular calcium concentration followed by fixation are compatible with a model in which CDH23 unfolds and/or with an excitatory displacement of the bundle as the calcium concentration gets lower.

Acknowledgments—Work supported by the Wellcome Trust, Deafness Research UK (D.N.F., C.M.H.), Tohoku University School of Medicine (Y.K.) and Midlands Institute of Otology (B.N.K.). Thanks are due to Karen Walker for technical assistance and Deborah Zetes for some of the material.

REFERENCES

Ahmed ZM, Goodyear R, Riazuddin S, Lagziel A, Legan PK, Behra M, Burgess SM, Lilley KS, Wilcox ER, Riazuddin S, Griffith AJ, Frolenkov GI, Belyantseva IA, Richardson GP, Friedman TB (2006) The tip-link antigen, a protein associated with the transduction complex of sensory hair cells, is protocadherin-15. J Neurosci 26:7022–7034.

Assad JA, Corey DP (1992) An active motor model for adaptation by vertebrate hair cells. J Neurosci 12:3291–3309.

Assad JA, Shepherd DM, Corey DP (1991) Tip link integrity and mechanical transduction in vertebrate hair cells. Neuron 7: 985–994.

Bagger-Sjöbäck D, Wersäll J (1973) The sensory hairs and tectorial membrane of the basilar papilla in the lizard *Calotes versicolor*. J Neurocytol 2:329–350.

Corey DP, Hudspeth AJ (1979) Ionic basis of the receptor potential in a vertebrate hair cell. Nature 281:675–677.

Corey DP, Hudspeth AJ (1983) Kinetics of the receptor current in bullfrog saccular hair cells. J Neurosci 3:962–976.

Crawford AC, Evans MG, Fettiplace R (1989) Activation and adaptation of transducer currents in turtle hair cells. J Physiol 419: 405–434.

Denk W, Holt JR, Shepherd GM, Corey DP (1995) Calcium imaging of single stereocilia in hair cells: localization of transduction channels at both ends of tip links. Neuron 15:1311–1321.

Flock Å, Flock B, Murray E (1977) Studies on the sensory hairs of receptor cells in the inner ear. Acta Otolaryngol 83:85–91.

Furness DN, Hackney CM (1985) Cross-links between stereocilia in the guinea pig cochlea. Hear Res 18:177–188.

Furness DN, Hackney CM (1986) High-resolution scanning-electron microscopy of stereocilia using the osmium-thiocarbohydrazide coating technique. Hear Res 21:243–249.

Furness DN, Hackney CM (2006) The structure and composition of the stereociliary bundle of vertebrate hair cells. In: Springer handbook of auditory research (Eatock RA, Fay R, Popper AN, eds), pp 95–153. Berlin/Heidelberg: Springer Science + Business Media.

Furness DN, Karkanevatos A, West B, Hackney CM (2002) An immunogold investigation of the distribution of calmodulin in the apex of cochlear hair cells. Hear Res 173:10–20.

Garcia JA, Yee AG, Gillespie PG, Corey DP (1998) Localization of myosin-Ibeta near both ends of tip links in frog saccular hair cells. J Neurosci 18:8637–8647.

Goodyear R, Richardson G (1992) Distribution of the 275 kD hair cell antigen and cell surface specialisations on auditory and vestibular hair bundles in the chicken inner ear. J Comp Neurol 325:243–256.

Hackney CM, Furness DN (1995a) Mechanotransduction in vertebrate hair cells: structure and function of the stereociliary bundle. Am J Physiol 268:C1–C13.

Hackney CM, Furness DN (1995b) Hair cell ultrastructure and mechanotransduction: morphological effects of low extracellular calcium levels on stereociliary bundles in the turtle cochlea. In: Active hearing (Flock A, Ottoson D, Ulfendahl M, eds), pp 103–111. Amsterdam: Elsevier Science Publishing Co.

Hackney CM, Furness DN, Benos DJ, Woodley JF, Barratt J (1992) Putative immunolocalization of the mechanoelectrical transduction channels in mammalian cochlear hair cells. Proc Biol Sci 248: 215–221.

Heywood P, Resnick S (1981) Application of the thiocarbohydrazide-osmium coating technique to scanning electron microscopy of the inner ear. Acta Otolaryngol 91:183–187.

Hudspeth AJ, Gillespie PG (1994) Pulling springs to tune transduction: adaptation by hair cells. Neuron 12:1–9.

Kachar B, Parakkal M, Kurc M, Zhao Y, Gillespie PG (2000) High-resolution structure of hair-cell tip links. Proc Natl Acad Sci U S A 97:13336–13341.

Kazmierczak P, Sakaguchi H, Tokita J, Wilson-Kubalek EM, Milligan RA, Muller U, Kachar B (2007) Cadherin 23 and protocadherin 15 interact to form tip-link filaments in sensory hair cells. Nature 449:87–91.

Neugebauer D-C (1986) Interconnections between the stereovilli of the fish inner ear: III. Indications for developmental changes. Cell Tissue Res 246:447–453.

Neugebauer D-C, Thurm U (1987) Surface charges of the membrane and cell adhesion substances determine the structural integrity of hair bundles from the inner ear of fish. Cell Tissue Res 249: 19–207.

Osborne MP, Comis SD, Pickles JO (1988) Further observations on the fine structure of tip links between stereocilia of the guinea pig cochlea. Hear Res 35:99–108.

Patel SD, Chen CP, Bahna F, Honig B, Shapiro L (2003) Cadherin-mediated cell-cell adhesion: sticking together as a family. Curr Opin Struct Biol 13:690–698.

Pickles JO, Comis SD, Osborne MP (1984) Cross-links between stereocilia in the guinea pig organ of Corti, and their possible relation to sensory transduction. Hear Res 15:103–112.

Ricci AJ, Fettiplace R (1997) The effects of calcium buffering and cyclic AMP on mechano-electrical transduction in turtle auditory hair cells. J Physiol 501:111–124.

Ricci AJ, Wu YC, Fettiplace R (1998) The endogenous calcium buffer and the time course of transducer adaptation in auditory hair cells. J Neurosci 18:8261–8277.

Rzadzinska AK, Schneider ME, Davies C, Riordan GP, Kachar B (2004) An actin molecular treadmill and myosins maintain stereocilia functional architecture and self-renewal. J Cell Biol 164:887–897.

Siemens J, Lillo C, Dumont RA, Reynolds A, Williams DS, Gillespie PG, Muller U (2004) Cadherin 23 is a component of the tip link in hair-cell stereocilia. Nature 428:950–955.

Sotomayor M, Corey DP, Schulten K (2005) In search of the hair-cell gating spring elastic properties of ankyrin and cadherin repeats. Structure 13:669–682.

Stafford WF, Walker ML, Trinick JA, Coluccio LM (2005) Mammalian class I myosin, Myo1b, is monomeric and cross-links actin filaments as determined by hydrodynamic studies and electron microscopy Biophys J 88:384–391.

Steyger PS, Gillespie PG, Baird RA (1998) Myosin Ibeta is located at tip link anchors in vestibular hair bundles. J Neurosci 18: 4603–4615.

Tsuprun V, Santi P (2000) Helical structure of hair cell stereocilia tip links in the chinchilla cochlea. J Assoc Res Otolaryngol 1: 224–231.

Tsuprun V, Goodyear RJ, Richardson GP (2004) The structure of tip links and kinocilial links in avian sensory hair bundles. Biophys J 87:4106–4112.

Unwin N (2003) Structure and action of the nicotinic acetylcholine receptor explored by electron microscopy. FEBS Lett 555:91–95.

(Accepted 12 February 2008)
(Available online 19 February 2008)